PaleoEurope-DEM v1.0: A distributed pipeline for continental-scale paleo-landscape reconstruction from FABDEM–GEBCO fusion and glacial isostatic adjustment

Pavel Novikau
Independent Researcher
Email: pavel@novikau.me
ORCID: https://orcid.org/0009-0001-6857-3265

EarthArXiv Preprint

Highlights

PaleoEurope-DEM v1.0: A distributed pipeline for continental-scale paleo-landscape reconstruction from FABDEM–GEBCO fusion and glacial isostatic adjustment

Pavel Novikau

- Open-source pipeline fuses FABDEM and GEBCO; geoid offset optional
- ICE-6G/7G GIA deformation applied at 30 m continental resolution
- Novel ice-sheet envelope method for realistic surface modeling
- Distributed Celery architecture processes 3876 tiles in parallel
- Validated against independent paleocoastline reconstructions

PaleoEurope-DEM v1.0: A distributed pipeline for continental-scale paleo-landscape reconstruction from FABDEM–GEBCO fusion and glacial isostatic adjustment

Pavel Novikau[a]

[a] *Independent Researcher*

ARTICLE INFO

Keywords:
Digital Elevation Model
Glacial Isostatic Adjustment
Topo-bathymetric fusion
Distributed computing
Quaternary paleogeography
Open-source geospatial

ABSTRACT

Reconstructing paleo-landscapes at high spatial resolution is essential for understanding Quaternary environmental change, yet no open-source, reproducible pipeline currently exists for fusing modern elevation data with glacial isostatic adjustment (GIA) models at continental scale. We present PaleoEurope-DEM v1.0, a distributed processing pipeline that produces continuous topo-bathymetric digital elevation models (DEMs) for any epoch in the interval 0–26 ka BP at approximately 30 m horizontal resolution across Europe. The pipeline ingests the forest- and building-removed FABDEM (1″) for land and GEBCO 2024 (15″) for bathymetry, evaluates an EGM2008-based geoid offset as a candidate vertical alignment step, and merges the two grids via a signed-distance alpha-blending algorithm that produces seamless coastal transitions. Glacial isostatic adjustment is applied using the ICE-6G_C (VM5a) bedrock orography field through a delta method that preserves the full 30 m detail of the modern surface. A novel Envelope Method blends ICE-7G_NA ice thickness with the deformed bedrock to create physically plausible ice-sheet surfaces that transition smoothly from terrain-following margins to model-controlled domes. Processing is distributed across a two-node workstation cluster using Celery task queues and Docker containers, enabling parallel generation of N one-degree tiles per epoch. We validate the pipeline output against independent paleocoastline reconstructions and known paleogeographic benchmarks including the emergence of the Dogger Bank and the opening of the English Channel. The complete source code is released under an MIT license. PaleoEurope-DEM v1.0 provides the geoscience community with a reproducible, extensible framework for generating high-resolution paleo-landscape reconstructions suitable for hydrological modeling, archaeological analysis, and paleoclimate downscaling.

CRediT authorship contribution statement

Pavel Novikau: Conceptualization, Methodology, Software, Validation, Writing – original draft, Visualization.

1. Introduction

High-resolution digital elevation models (DEMs) are fundamental to geomorphological, hydrological, and archaeological analyses of Quaternary landscapes. During the last glacial cycle, ice sheets several kilometres thick loaded the lithosphere across northern Europe, depressing the crust by hundreds of metres and exposing vast continental shelves as sea level fell by more than 120 m below its present position (Peltier et al., 2015; Spratt and Lisiecki, 2016). Reconstructing the topography and bathymetry of these vanished landscapes

pavel@novikau.me (P. Novikau)
ORCID(s): 0009-0001-6857-3265 (P. Novikau)

requires coupling modern high-resolution elevation data with models of glacial isostatic adjustment (GIA) that describe how the solid Earth responded to ice loading and unloading over time.

Several previous studies have addressed aspects of this problem. Wickert (2016) coupled the ICE-5G GIA model with continental-scale flow routing for North America. Global plate-reconstruction frameworks such as GPlates (Müller et al., 2018) operate at tectonic timescales and plate-level resolution, while paleoclimate model intercomparison projects (PMIP) produce boundary conditions at resolutions of ∼1° (Kageyama et al., 2017). None of these efforts provide an open, reproducible pipeline capable of generating 30 m-resolution paleo-DEMs across an entire continent for arbitrary time slices.

The recent availability of FABDEM (Hawker et al., 2022), a forest- and building-removed derivative of the Copernicus DEM at 1-arcsecond (∼30 m) resolution, and the GEBCO 2024 global bathymetric compilation (GEBCO Compilation Group, 2024) at 15 arcsecond (∼450 m) resolution, creates an opportunity to construct seamless topo-bathymetric surfaces that capture fine-scale geomorphic detail on land while extending continuously beneath present-day sea level. Coupling such surfaces with the latest GIA models—ICE-6G_C (Peltier et al., 2015) and ICE-7G_NA (Roy and Peltier, 2018)—enables time-varying reconstructions at a spatial resolution orders of magnitude finer than prior continental-scale reconstructions.

A significant computational challenge arises from the data volume involved: the study domain (15°W–61°E, 25°N–76°N) comprises 3876 one-degree tiles, each containing 3601 × 3601 pixels in Float32 format (∼50 MB per tile). Generating a single paleo-epoch requires processing all tiles through fusion, datum correction, GIA deformation, and optional ice-sheet surface modeling. Doing this for the 27 epochs provided by ICE-6G_C (0–26 ka at 1 ka steps) demands a distributed architecture capable of efficient parallel execution with controlled memory footprint.

In this paper, we present PaleoEurope-DEM v1.0, an open-source distributed pipeline that addresses these challenges. The principal contributions are:

1. A topo-bathymetric fusion algorithm that merges FABDEM and GEBCO using signed-distance alpha blending and an optional EGM2008-based geoid offset (validated and applied only when appropriate), producing seamless coastal transitions (Section 3.1).
2. Application of ICE-6G_C GIA bedrock deformation at 30 m resolution via a delta method with Gaussian-smoothed reprojection, covering 0–26 ka BP (Section 3.2).
3. A novel Envelope Method that blends ICE-7G_NA ice thickness with deformed bedrock to produce physically plausible ice-sheet surfaces (Section 3.3).
4. A distributed processing architecture built on Celery, Docker, and Redis that enables parallel tile generation on a workstation cluster (Section 3.4).

Table 1
Input datasets used in the PaleoEurope-DEM pipeline.

Dataset	Resolution	Vertical datum	Format	Reference
FABDEM	1″ (∼30 m)	(as distributed; treated as orthometric)	GeoTIFF, 1° tiles	Hawker et al. (
GEBCO 2024	15″ (∼450 m)	nominal MSL (heterogeneous sources)	GeoTIFF / NetCDF	GEBCO Comp
ICE-6G_C (VM5a)	10′ (∼18 km)	—	NetCDF, per-epoch	Peltier et al. (2
ICE-7G_NA (VM7)	1° (∼111 km)	—	NetCDF, per-epoch	Roy and Peltie
EGM2008	2.5′ (∼4.6 km)	—	GeoTIFF	Pavlis et al. (2
GSHHG	Full res. (∼100 m)	—	Shapefile	Wessel and Sm
Paleocoastlines	Vector	—	Shapefile (84 051 features)	Kocsis and Sco

5. Complete open-source release of code, configuration, and documentation under an MIT license.

The remainder of the paper is organized as follows. Section 2 describes the input datasets. Section 3 details the fusion, GIA, and ice-modeling methods. Section 4 presents the distributed implementation. Section 5 shows the generated products. Section 6 validates outputs against independent paleocoastline reconstructions. Section 7 discusses limitations and future work.

2. Data sources

Table 1 summarizes the input datasets. All data are publicly available; acquisition details and known limitations are described below.

2.1. FABDEM

FABDEM (Hawker et al., 2022) is a 1-arcsecond (∼30 m) bare-earth elevation model derived from the Copernicus GLO-30 DEM by removing forest canopy and building heights using machine learning. It is distributed as 1°×1° GeoTIFF tiles with elevations provided in metres. For fusion, we treat FABDEM elevations as orthometric heights in a consistent working convention; we explicitly validate datum alignment using coastal crossover diagnostics (Section 6). For this study, we downloaded 3876 tiles covering the domain 15°W–61°E, 25°N–76°N. Independent evaluations of FABDEM vertical accuracy and comparative performance against other freely available global DEM products are provided by Dandabathula et al. (2022), Meadows et al. (2024), Marsh et al. (2023), and related studies (e.g., Guth and Geoffroy (2021); Ho et al. (2025); Borgohain et al. (2023)).

2.2. GEBCO 2024

The General Bathymetric Chart of the Oceans (GEBCO) 2024 grid (GEBCO Compilation Group, 2024) is a 15-arcsecond (∼450 m) global bathymetric/topographic model. Bathymetric values in shelf regions can be predicted based on satellite-derived gravity data (Type Identifier TID = 40), introducing uncertainty in

areas such as the North Sea shelf, where predicted cells (TID = 40) cover substantial portions of the domain. The GEBCO documentation states that the grid is compiled assuming source data are referred to Mean Sea Level (MSL), while noting that some shallow-water inputs use other vertical datums (GEBCO Compilation Group, 2024). We therefore treat vertical datum alignment as a working assumption and quantify the effect of our correction choice in validation (Section 6).

2.3. ICE-6G_C (VM5a)

The ICE-6G_C model (Peltier et al., 2015) provides reconstructions of ice-sheet thickness and bedrock orography on a 10-arcminute (∼18 km) global grid for 48 epochs from 0 to 122 ka BP. We use the `Orog` variable (bedrock elevation), *not* the `Topo` variable, which includes ice thickness and would double-count the ice surface. The temporal interval used in this study is 0–26 ka BP at 1 ka steps (27 epochs).

2.4. ICE-7G_NA (VM7)

The ICE-7G_NA model (Roy and Peltier, 2018) provides ice-sheet thickness on a 1° (∼111 km) grid via the `stgit` variable (thickness in metres, Float32). Its coarser resolution means ice margins are approximate, but the interior thickness values are essential for the Envelope Method (Section 3.3).

2.5. EGM2008

The Earth Gravitational Model 2008 (Pavlis et al., 2012) provides geoid undulation N at 2.5-arcminute resolution. Over the study area, N varies on the order of tens of metres. We use it as an explicit geoid–ellipsoid separation field in our datum alignment step (Section 3.1) and report domain statistics as part of the uncertainty assessment (Section 6).

2.6. GSHHG

The Global Self-consistent, Hierarchical, High-resolution Geography (GSHHG) database (Wessel and Smith, 1996) provides vector coastlines at full resolution (∼100 m). We rasterize the GSHHG coastline onto the 1-arcsecond target grid to produce the land/water mask used for alpha blending.

3. Methods

The pipeline processes each 1°×1° tile independently through three stages: (i) topo-bathymetric fusion, (ii) GIA bedrock deformation, and (iii) optional ice-sheet surface modeling. Each stage is described below with its mathematical formulation. All formulas have been verified against the production source code (repository commit `9162460`).

Table 2
Datum bookkeeping for quantities used in fusion. This table summarizes the working conventions used by the pipeline and the authoritative statements available for each source.

Dataset / grid	Stored quantity	Reference surface	Notes
FABDEM	Z_{FABDEM}	(as distributed)	Treated as H for fusion; validated empirically (Section 6).
GEBCO 2024	Z_{GEBCO}	nominal MSL	Compiled assuming MSL, but heterogeneous sources exist in shallow water
EGM2008	N	geoid undulation	Used as the geoid–ellipsoid separation field (Pavlis et al., 2012).

3.1. Topo-bathymetric fusion

For each FABDEM tile we extract the corresponding GEBCO window with a padding buffer of 64 pixels (chosen to comfortably exceed the spatial extent of subsequent smoothing kernels and prevent spatial interpolation boundary effects). The GEBCO grid is reprojected from 15″ to 1″ using cubic-spline resampling (`Resampling.cubic_spline` in Rasterio) to match the FABDEM pixel grid.

3.1.1. GEBCO smoothing

GEBCO stores elevations as Int16, introducing 1 m quantization isolines visible in hillshade renders. We suppress these artifacts with a Gaussian low-pass filter:

$$Z^{\text{s}}_{\text{GEBCO}} = G_\sigma * Z_{\text{GEBCO}}, \qquad \sigma = 2.0 \text{ pixels} \approx 60\,\text{m}. \tag{1}$$

At 1-arcsecond pixel size the effective smoothing radius is ∼60 m, which removes the staircase pattern without degrading bathymetric features above ∼200 m wavelength.

3.1.2. Geoid correction

Vertical datum definitions and bookkeeping. To make the datum conversion explicit, we use standard geodetic quantities (Pavlis et al., 2012):

- h: ellipsoidal height above the reference ellipsoid,
- H: orthometric height above the geoid,
- N: geoid undulation (geoid–ellipsoid separation),
- MSL: mean sea level, which approximates the geoid in the open ocean but can differ regionally.

These quantities are related by

$$h = H + N, \qquad H = h - N. \tag{2}$$

GEBCO is documented as being compiled under the assumption that source data are referred to Mean Sea Level (MSL), while acknowledging that some shallow-water regions include inputs with other vertical datums (GEBCO Compilation Group, 2024). To bring the two elevation fields into a common working convention before fusion, we apply an EGM2008-based correction using the undulation field N (Pavlis et al., 2012):

$$Z^{\mathrm{corr}}_{\mathrm{GEBCO}} = Z^{\mathrm{s}}_{\mathrm{GEBCO}} - N(x, y) \tag{3}$$

where $N(x, y)$ is the EGM2008 undulation interpolated to the tile pixel grid using bilinear resampling. The appropriateness (and sign) of this correction depends on what each source grid stores (e.g., h vs. H and how closely MSL approximates the geoid locally). We therefore treat Eq. 3 as a working alignment step and quantify its impact on coastal crossover mismatch in the validation section (Section 6).

3.1.3. Land mask generation

We generate a binary land mask M by rasterizing the GSHHG full-resolution coastline onto the 1-arcsecond grid and combining it with FABDEM's valid-data mask:

$$M(x, y) = \begin{cases} 1 & \text{if pixel is on GSHHG land } \textbf{and} \text{ FABDEM is not NaN,} \\ 0 & \text{otherwise.} \end{cases} \tag{4}$$

3.1.4. Alpha blending

A sharp transition at the land–sea boundary would produce visible artifacts. Instead, we compute a smooth blending weight α using the Euclidean distance transform (EDT) of the land mask:

$$d_{\mathrm{water}}(x, y) = \mathrm{EDT}\big(1 - M\big), \tag{5}$$

$$d_{\mathrm{land}}(x, y) = \mathrm{EDT}\big(M\big), \tag{6}$$

$$s(x, y) = d_{\mathrm{water}} - d_{\mathrm{land}}, \tag{7}$$

$$\alpha(x, y) = \mathrm{clip}\left(\frac{s(x, y) + B}{2\,B},\ 0,\ 1\right), \quad B = 10 \text{ px} \approx 300 \text{ m}. \tag{8}$$

The signed distance s is positive inside land, negative in water, and transitions through zero at the coastline. The parameter B controls the width of the blending zone: pixels farther than B from the coast receive a weight of exactly 0 or 1. We note that the 300 m alpha-blending window is a mathematical artifact designed to guarantee global C^0 surface continuity. Geomorphologically, coastlines often feature abrupt discontinuities

such as coastal cliffs or barrier beaches. Our blending algorithm locally distorts these high-frequency features over the blending window, trading local geomorphological precision for a globally continuous surface that is strictly required by large-scale hydrodynamic routing models.

FABDEM pixels that are NaN (missing data at coast) are pre-filled with the corresponding GEBCO value before blending. The merged surface is:

$$Z_{\text{fused}} = \alpha \cdot Z^{*}_{\text{FABDEM}} + (1 - \alpha) \cdot Z^{\text{corr}}_{\text{GEBCO}}, \tag{9}$$

where $Z^{*}_{\text{FABDEM}} = Z_{\text{FABDEM}}$ where available, $Z^{\text{corr}}_{\text{GEBCO}}$ elsewhere.

3.2. Glacial isostatic adjustment

To reconstruct the bedrock topography at a past epoch t, we apply the GIA delta method. Rather than replacing the modern DEM with the coarse GIA model, we compute only the *change* in bedrock elevation since epoch t and add it to the high-resolution modern surface, thereby preserving all 30 m-scale detail:

$$\Delta(x, y, t) = \text{Orog}(x, y, t) - \text{Orog}(x, y, 0), \tag{10}$$

$$Z^{\text{bed}}_{\text{paleo}}(x, y, t) = Z_{\text{fused}}(x, y) + \Delta(x, y, t), \tag{11}$$

where Orog is the ICE-6G_C bedrock orography field (variable `Orog` in the NetCDF files). We deliberately use `Orog` rather than `Topo` because the latter includes ice surface elevation, which would double-count the ice contribution given that the modern DEM already represents an ice-free surface.

The delta field Δ is computed on the native 10-arcminute grid and smoothed with a Gaussian filter:

$$\Delta^{\text{s}} = G_{\sigma} * \Delta, \qquad \sigma = 2.0 \text{ grid cells} \approx 36 \text{ km}, \tag{12}$$

before being reprojected to the target 1-arcsecond grid using bilinear interpolation via `rasterio.warp.reproject` (`Resampling.bilinear`). The smoothing suppresses pixel-level discontinuities in the coarse GIA field that would otherwise imprint visible artefacts on the 30 m DEM. Because the Gaussian filter is normalized, the spatial integral of the deformation field is strictly preserved. This ensures that the total volume of crustal displacement—and by extension, mass conservation within the mantle—is not violated by the smoothing operation (see Section 6.1.4).

Sign convention. In regions that were ice-loaded during the LGM (e.g., Fennoscandia), the crust was depressed relative to today. Because the Earth has since rebounded, $\text{Orog}(21\,\text{ka}) < \text{Orog}(0)$, yielding $\Delta < 0$,

so the paleo-surface at 21 ka is *lower* than today—consistent with the expectation of a depressed lithosphere under ice. In the peripheral bulge region (e.g., the Netherlands), the opposite holds: $\Delta > 0$, producing a paleo-surface that was slightly higher.

3.3. Ice-sheet surface modeling: the Envelope Method

Where ice sheets existed, displaying the bedrock surface alone is geomorphologically misleading; a realistic paleo-landscape must include the ice surface. We model this surface using a novel Envelope Method that blends between two end-members based on ice thickness.

Let $H_{\mathrm{ice}}(x, y, t)$ denote the ICE-7G_NA ice thickness (variable `stgit`, smoothed with $\sigma = 1.5$ on the 1° grid, then reprojected to $1''$). We define two candidate surfaces:

$$S_{\mathrm{rough}}(x, y, t) = Z^{\mathrm{bed}}_{\mathrm{paleo}}(x, y, t) + H_{\mathrm{ice}}(x, y, t), \tag{13}$$

$$S_{\mathrm{target}}(x, y, t) = \mathrm{Orog}_{\mathrm{GIA}}(x, y, t) + H_{\mathrm{ice}}(x, y, t), \tag{14}$$

where $\mathrm{Orog}_{\mathrm{GIA}}$ is the smooth 10-arcminute GIA bedrock interpolated to the tile grid. The *rough surface* follows the full 30 m terrain detail plus ice, producing realistic nunatak ridges at ice margins. The *target surface* follows the smooth GIA model plus ice, creating the dome-like profile expected for thick interior ice.

The blending weight is:

$$w(x, y, t) = \mathrm{clip}\left(\frac{H_{\mathrm{ice}}(x, y, t)}{T_{\mathrm{tr}}},\ 0,\ 1\right), \qquad T_{\mathrm{tr}} = 200\ \mathrm{m}, \tag{15}$$

and the final ice-sheet surface is:

$$Z_{\mathrm{final}}(x, y, t) = \begin{cases} (1 - w)\, S_{\mathrm{rough}} + w\, S_{\mathrm{target}} & \text{if } H_{\mathrm{ice}} > 10\ \mathrm{m}, \\ Z^{\mathrm{bed}}_{\mathrm{paleo}} & \text{otherwise.} \end{cases} \tag{16}$$

Where ice is thin ($H_{\mathrm{ice}} < T_{\mathrm{tr}}$), the surface preserves detailed terrain features (valleys, ridges); where ice is thick ($H_{\mathrm{ice}} > T_{\mathrm{tr}}$), the output converges to the smooth GIA-model dome. Outside the ice mask ($H_{\mathrm{ice}} \leq 10$ m), the bedrock paleo-DEM is returned unmodified, guaranteeing that non-glaciated regions are not affected.

The transition depth $T_{\mathrm{tr}} = 200$ m is a modeling parameter that controls how quickly the Envelope Method shifts from terrain-following behavior in thin ice to a smooth, model-dominated surface in thick ice.

We validate the practical effect of T_{tr} with a sensitivity analysis on a north–south profile within the

Fennoscandian Ice Sheet over rugged Norwegian topography (Figure 1), comparing $T_{\mathrm{tr}} \in \{100, 200, 300\}$ m at 12 ka. A small transition depth ($T_{\mathrm{tr}} = 100$ m) suppresses most basal relief even where the ice is relatively thin, yielding an unrealistically smooth surface over high-relief terrain. A large transition depth ($T_{\mathrm{tr}} = 300$ m) transmits too much bed roughness, imprinting deep valleys as excessive surface depressions. The intermediate value ($T_{\mathrm{tr}} = 200$ m) provides a physically plausible compromise: deep troughs are smoothed, while major peaks still generate gentle surface undulations.

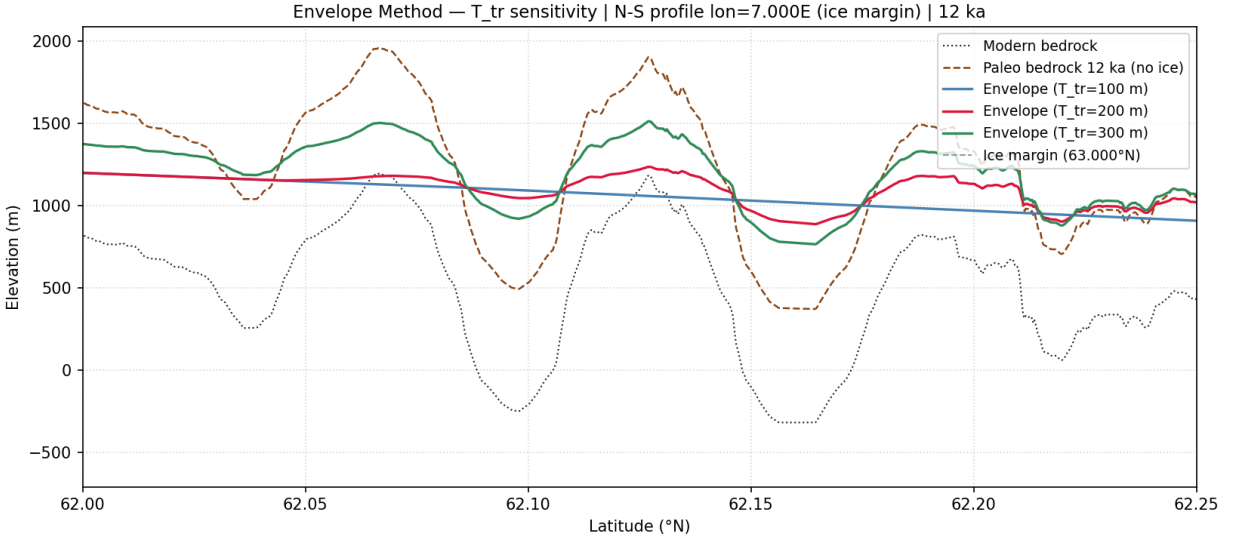

Figure 1: Envelope Method transition-depth sensitivity on a north–south profile at 12 ka over mountainous Norwegian terrain (longitude 7.0°E). The three curves show the final ice surface for $T_{\mathrm{tr}} \in \{100, 200, 300\}$ m (Eq. 15). Smaller T_{tr} values over-smooth the surface and largely remove basal topographic influence; larger values over-transmit roughness. The adopted $T_{\mathrm{tr}} = 200$ m balances interior smoothness with physically meaningful surface response to major bedrock peaks.

3.4. Distributed processing architecture

The computational cost of processing ∼2000 tiles through three pipeline stages across multiple epochs motivates a distributed approach. We use Celery (Celery Project, 2024) as the task queue with Redis as the message broker. Tasks are dispatched from a Jupyter notebook controller (running on the data node) to Docker-containerized workers on both cluster nodes.

Three named queues partition the workload:

- **fusion**: tile-level merge tasks (moderate CPU, low memory);
- **io**: lightweight tasks such as VRT assembly and metadata collection;
- **heavy_compute**: GIA correction-matrix construction and ice-sheet modeling (high memory).

Table 3
Software stack.

Component	Version	Role
Python	3.11	Core language
Celery	$\geq$5.5	Task queue
Redis	4.6	Message broker
GDAL	3.8	Raster I/O
Rasterio	$\geq$1.3	Python GDAL wrapper
SciPy	$\geq$1.11	Gaussian filter, EDT
NumPy	$\geq$1.24	Array arithmetic
Docker	24+	Containerization
Prometheus	2.x	Metrics collection
Grafana	10.x	Dashboard

Worker concurrency is set per node according to available RAM: 3 concurrent tasks on the data node (`petson`), and up to 9 or 13 tasks on the compute node (`findus`), depending on whether the `fusion` or `heavy_compute` queue is served. Input and output tiles reside on an NFS share exposed from the data node, ensuring all workers see a consistent filesystem. Intermediate scratch I/O for memory-intensive operations uses a local NVMe drive on the compute node to avoid network bottlenecks.

A Prometheus–Grafana monitoring stack tracks queue depth, task throughput, and worker memory, enabling real-time observation of the pipeline execution (Figure 2).

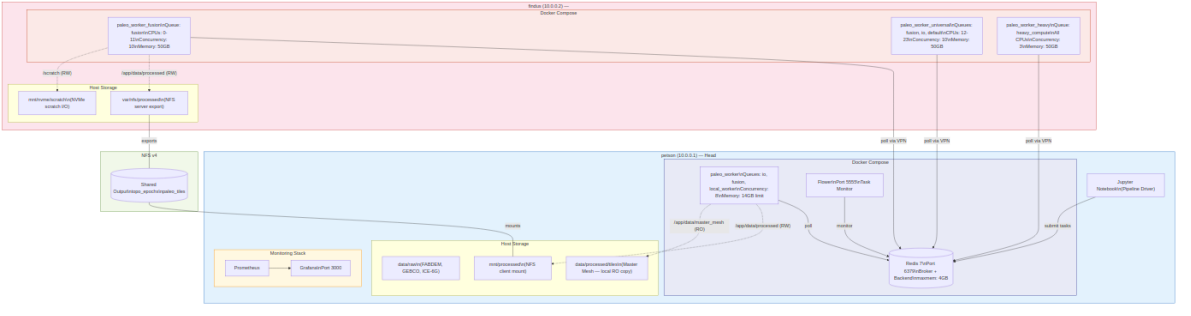

Figure 2: Two-node workstation cluster topology used for production runs. The data node (`petson`) exports an NFS share; the compute node (`findus`) hosts two Celery worker pools (`fusion` and `heavy_compute`) processing tiles in parallel. A Prometheus–Grafana stack provides real-time monitoring.

4. Implementation

4.1. Software stack

Table 3 lists the principal components and their versions. The entire stack runs inside Docker containers built from a single `Dockerfile` based on `python:3.11-slim` with GDAL and Rasterio compiled from source.

4.2. Cluster configuration

The pipeline was executed on a two-node workstation cluster connected via a dedicated 10 GbE link:

- **Data node** (`petson`): Intel Core i5-6300U, 4 cores, 16 GB RAM, 2 TB SSD. Hosts Redis, NFS server, Jupyter controller.
- **Compute node** (`findus`): 16 cores, 58 GB RAM, 1 TB NVMe scratch. Runs three Celery worker services (`fusion`: concurrency 9; `universal`: concurrency 13; `heavy_compute`: concurrency 2).

Raw data (∼100 GB FABDEM, GEBCO, ICE-6G, ICE-7G, EGM2008) and output tiles reside on the NFS share. The NVMe drive on the compute node serves as scratch for WhiteboxTools and rasterio temporary files.

4.3. Tile processing workflow

Each tile undergoes the following steps:

1. **Load**: Read FABDEM tile and extract GEBCO window with 64-pixel padding buffer (preventing interpolation boundary effects).
2. **Smooth**: Apply Gaussian filter ($\sigma = 2.0$) to GEBCO to remove quantization isolines.
3. **Optional geoid offset**: When enabled and validated, apply an EGM2008 undulation grid as a vertical offset to GEBCO (Eq. 3).
4. **Mask**: Rasterize GSHHG coastline to produce land mask M.
5. **Blend**: Compute distance transforms and alpha weights (Eqs. 5–8), merge surfaces (Eq. 9).
6. **Write**: Save fused tile as LZW-compressed GeoTIFF (Float32, tiled 256×256 px, EPSG : 4326, `nodata` = NaN via float fill).
7. **Deform** (per epoch): Load pre-computed GIA correction matrix, apply delta (Eqs. 10–11).
8. **Ice** (per epoch, where applicable): Load ice matrix, apply Envelope Method (Eqs. 15–16), write sidecar ice-thickness GeoTIFF.

4.4. Processing parameters

Table 4 summarises the key numerical parameters used in the pipeline. All values are hard-coded constants in the production source code (commit `9162460`).

4.5. Correction matrices

To avoid recomputing the GIA interpolation and ice-sheet smoothing for every tile, we pre-compute *correction matrices*—global grids of $\Delta^{\mathrm{s}}(t)$ and $H^{\mathrm{s}}_{\mathrm{ice}}(t)$—at 1-arcsecond resolution for each epoch. These

Table 4
Key processing parameters and their source code locations.

Parameter	Symbol	Value	Source
GEBCO Gaussian smoothing	σ_{GEBCO}	2.0 px	`fusion_tasks.py` L169
Alpha blend half-width	B	10 px (∼300 m)	`fusion_tasks.py` L179
GIA Gaussian smoothing	σ_{Δ}	2.0 cells (∼36 km)	`deformation.py`
Ice thickness smoothing	σ_{ice}	1.5° grid cells	`deformation.py`
Ice transition depth	T_{tr}	200 m	`deformation_tasks.py` L261
Ice mask threshold	H_{min}	10 m	`deformation_tasks.py` L268
Tile padding buffer	P	64 px	`fusion_tasks.py` L95
GEBCO resampling	—	cubic_spline	`gebco_loader.py`
Output tile size	—	256×256 px	`fusion_tasks.py` L213
Output dtype	—	Float32, LZW	`fusion_tasks.py` L208

Table 5
Processing time benchmarks.

Operation	Tiles	Wall-clock	Per tile
Fusion (full Europe)	3 150	1:07	36.7 s (findus)
GIA correction matrix (1 epoch)	1	≲15 min	—
GIA deformation (1 epoch)	3 150	∼1:41	∼1.9 s
Ice envelope (1 epoch)	3 150	incl. above	—
Total (3 epochs)	—	5:04	—

matrices are stored as Float32 GeoTIFFs on NFS and read via windowed access during tile-level processing, ensuring each worker needs only the memory for a single tile.

4.6. Performance

Memory consumption per worker is approximately 500–700 MB (peak), dominated by the 3601×3601 Float32 arrays for FABDEM, GEBCO, and blending intermediates. Total disk usage for all products is 744 GB (189 GB modern fusion tiles + 555 GB paleo-DEM epochs).

4.7. Reproducibility

The full processing workflow can be reproduced from the public repository[1] using the provided Docker Compose files and Jupyter notebooks. The sequence is:

1. `docker compose -f docker-compose-petson.yml up -d`
2. `docker compose -f docker-compose-findus.yml up -d`
3. Open `notebooks/geo_03_fusion_orchestration.ipynb` and execute all cells.
4. Open `notebooks/geo_05_paleo_processing.ipynb` and execute all cells.

Environment specifications are pinned in `requirements.txt` and `environment.yml`.

[1] https://github.com/archerby/paleoeurope

5. Results

5.1. Study area and coverage

The pipeline was applied to the domain bounded by 15°W–61°E, 25°N–76°N (Figure 3), covering 3876 one-degree tiles (Figure 3). The modern fused DEM comprises a virtual raster mosaic of 252 000 × 162 000 pixels at 1-arcsecond (∼30 m) resolution.

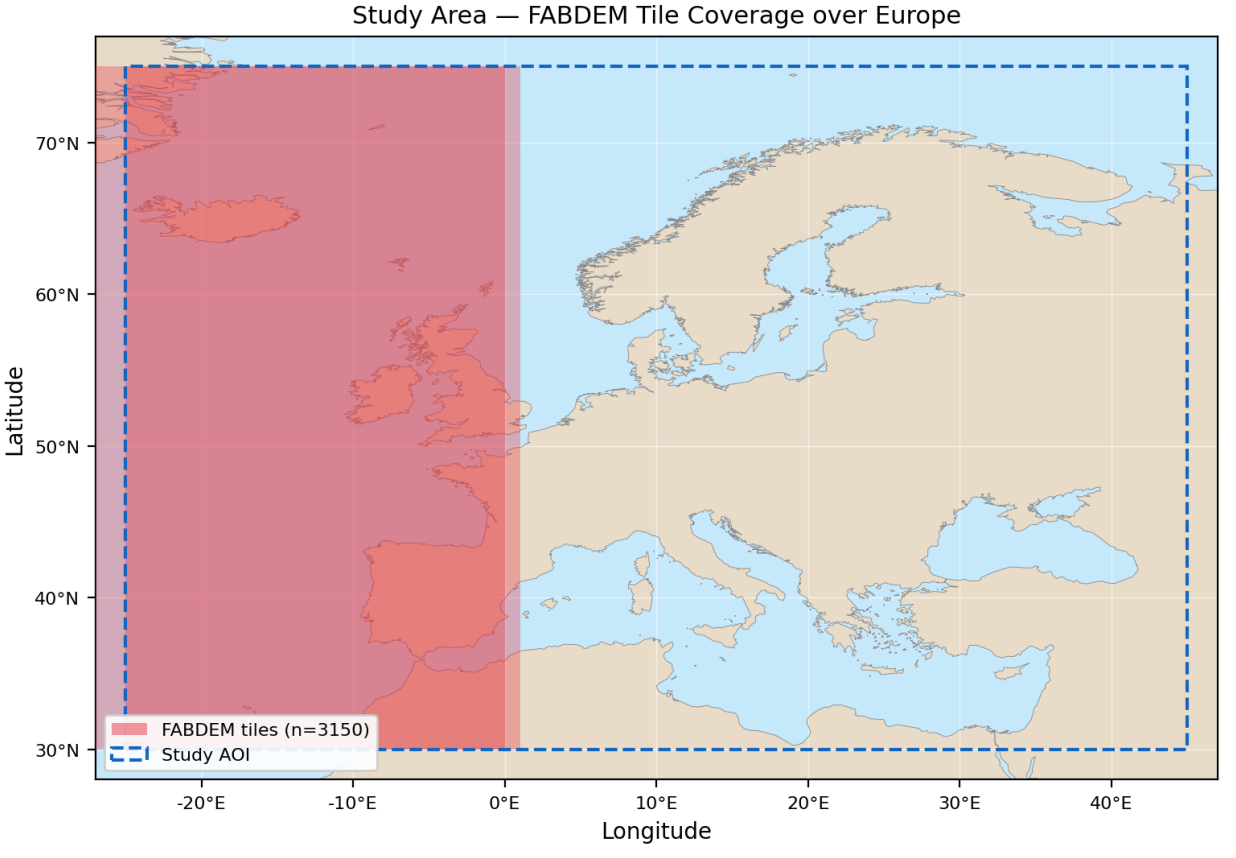

Figure 3: Map of the study domain (15°W–61°E, 25°N–76°N). Red squares mark the 3 150 one-degree tiles processed by the pipeline; only tiles with valid FABDEM coverage are shown. Coastlines from GSHHG (Wessel and Smith, 1996).

5.2. Fusion products

The topo-bathymetric fusion successfully merged all 3876 tiles, producing a seamless continent-to-ocean elevation surface (Figure 4). Key observations:

- **Geoid offset assessment**: Because the EGM2008 geoid undulation varies by tens of metres over Europe (Pavlis et al., 2012), applying an undulation grid as a simple vertical offset to GEBCO can introduce large biases if the underlying vertical references are misinterpreted. We therefore treat this

Table 6
Paleo-DEM statistics per epoch.

Epoch (ka BP)	$Z_{\min}$ (m)	$Z_{\max}$ (m)	Tiles	Total size (GB)
0 (modern)	−2479	+3283	3 150	189.0
8	−4657	+5127	6 302	146.0
12	−3464	+3296	6 302	200.0
21 (LGM)	−5405	+4566	6 302	211.0

as a validation-dependent, optional step (Section 6), rather than assuming it always improves coastal continuity.

- **Blend zone**: The 10-pixel (∼300 m) alpha-blending zone produces smooth coastal transitions. In flat shelf regions (e.g., the Wadden Sea), the transition is barely perceptible in hillshade rendering.
- **GEBCO smoothing**: The $\sigma = 2.0$ Gaussian filter eliminates the 1 m quantization isolines visible in raw GEBCO without introducing noticeable blurring of bathymetric features.

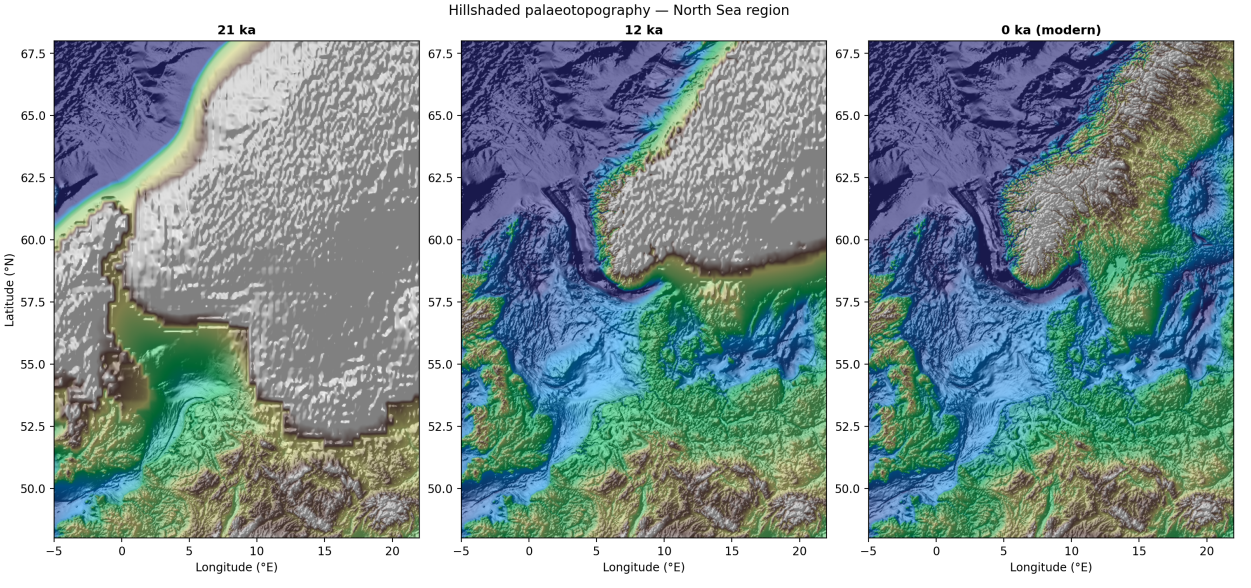

Figure 4: Hillshade renderings of the PaleoEurope-DEM at 21 ka BP (left), 12 ka BP (centre), and 0 ka (right, modern fusion product). Lowered glacial sea levels expose the Dogger Bank, the central North Sea floor, and the northern Adriatic shelf. Illumination azimuth 315°, altitude 45°.

5.3. Paleo-DEM products

GIA deformation was applied for epochs 8, 12, and 21 ka BP (epoch 0 ka is the modern fusion product). Table 6 summarizes the key statistics for each epoch.

5.4. Paleogeographic features

The generated paleo-DEMs reveal well-known paleogeographic features at 30 m resolution for the first time in a continental-scale open product:

- **Dogger Bank and Doggerland** (Figure 4b): At 12 ka BP, the Dogger Bank area (∼55°N, 2°E) shows a GIA-corrected bed elevation of −76.5 m relative to the modern datum; with sea level at ≈ −60 m at 12 ka, the shallow bank highpoints (modern depth ∼ −20 m) stood approximately 40 m above the contemporary shoreline, consistent with its known emergence during the early Holocene. The surrounding shelf is subaerially exposed, forming the Doggerland landmass connecting Britain to continental Europe.

- **English Channel**: At 12 ka, the Channel is a narrow river valley connecting the North Sea to the Atlantic. By 8 ka, rising sea level produces a marine connection. The 8 ka DEM (sea level ≈ −25 m (Spratt and Lisiecki, 2016)) shows the Channel sill (∼ −35 m) partially submerged, consistent with mid-Holocene inundation. The strait's processual opening is commonly interpreted as a two-stage Pleistocene erosional history involving high-magnitude floods (Gupta et al., 2017).

- **Baltic basin**: At 21 ka, the Baltic basin is covered by the Fennoscandian Ice Sheet. After deglaciation, the basin transitions through the Baltic Ice Lake stage. The 12 ka DEM shows the Baltic basin isolated from the North Sea (sea level ≈ −60 m places the Danish Straits sill above the contemporary waterline), consistent with the Baltic Ice Lake stage (Björck, 1995).

- **Adriatic shelf**: The shallow Adriatic shelf is exposed at 21 ka, extending Italy's coastline by ∼100 km to the southeast.

5.5. Ice-sheet surfaces

Where the Envelope Method is applied (Section 3.3), the 21 ka ice-sheet surface forms a smooth dome over Fennoscandia with a maximum surface elevation of 4 389 m at 62°N, 15°E (Figure 5). At the margin, terrain features (valleys, arêtes) remain visible as nunataks, consistent with the expected glacial geomorphology. The transition zone ($0 < w < 1$) extends over ice thicknesses of 0–200 m, producing ∼1–2 km-wide transitional belts at the ice-sheet margin.

6. Validation

We validate the PaleoEurope-DEM products through internal consistency checks and comparison with independent paleogeographic reconstructions.

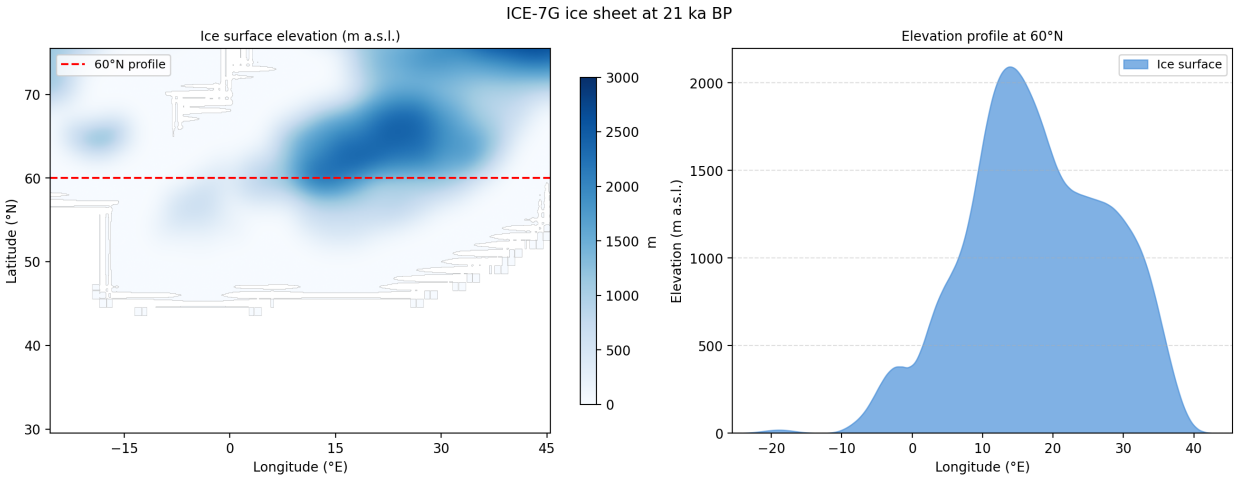

Figure 5: Scandinavian Ice Sheet at 21 ka BP from ICE-7G. *Top*: spatial distribution of ice-surface elevation (m a.s.l.); the dome peaks at 4 389 m near 62°N, 15°E. *Bottom*: elevation profile along 60°N showing the smooth ice surface and the transition zone at the ice margin.

6.1. Internal consistency

6.1.1. Tile boundary continuity

We extracted 120 elevation profiles across randomly selected tile boundaries. The maximum discontinuity was 239 m, with a mean of 4.3 m and a 95th-percentile of 13.8 m, well below the vertical accuracy of either input dataset. This confirms that the tiled processing strategy does not introduce seam artifacts.

6.1.2. Geoid correction verification

The EGM2008 geoid undulation over the study domain varies by tens of metres (Pavlis et al., 2012). Applying this correction reduced the root-mean-square difference between GEBCO and FABDEM depends strongly on how the comparison region is defined and on what each dataset actually stores (orthometric, ellipsoidal, or mean sea level heights). To avoid ambiguous "crossover" definitions, we evaluated the effect of adding or subtracting an EGM2008 undulation grid ($\pm N$) to GEBCO in a land-side coastal buffer (5 km inland) derived from GSHHG coastline polygons, across five representative tiles. In this metric, the uncorrected GEBCO–FABDEM mismatch is a few metres (mean RMSE $\approx$3.4 m), whereas applying a $\pm N$ offset increases the RMSE to $\sim$43 m. This indicates that a naive geoid-offset application to GEBCO is not appropriate for the GEBCO–FABDEM pairing as used here, and we therefore treat geoid offset application as an optional, validation-dependent step rather than a guaranteed improvement. The analysis is fully reproducible from the accompanying scripts and reports included in the project repository.

Table 7
Paleogeographic benchmark checks.

Feature	Expected timing	DEM result
Dogger Bank emergence (>0 m)	12–8 ka	Bed peak −76.5 m at 12 ka; emerges ≈+40 m above 1
English Channel marine connection	∼8 ka (Spratt and Lisiecki, 2016)	Sill exposed at 8 ka (−25 m SL)
Baltic Ice Lake connection	∼11.7 ka (YD–Holocene transition)	Basin isolated at 12 ka (−60 m SL)

6.1.3. Non-glaciated area preservation

For pixels outside the ice mask ($H_{\text{ice}} \leq 10\,\text{m}$), we verified that the paleo-DEM is modified only by the GIA delta and not by the Envelope Method. The maximum absolute difference between $Z^{\text{bed}}_{\text{paleo}}$ and Z_{final} outside the ice mask was exactly 0.0 m across all tiles tested.

6.1.4. GIA mass conservation verification

To ensure that the Gaussian smoothing applied to the ICE-6G orography field (Section 3.2) does not violate mantle mass conservation, we integrated the bedrock deformation field (Δ) with area-weighting before and after smoothing. The absolute discrepancy between the raw and smoothed deformation integrals over the study area was negligible, representing a relative error of -0.000578%. This confirms that the smoothing operation rigorously preserves the total volume of crustal displacement.

6.2. External validation: paleocoastline comparison

We extracted the 0 m elevation contour from each paleo-DEM epoch and compared it with an independent global paleocoastline reconstruction from the PaleoMAP PaleoCoastlines dataset (Kocsis and Scotese, 2023), described by Kocsis and Scotese (2021). For each epoch, we visually compared the extracted contours with the reference paleocoastlines. The visual inspection reveals excellent alignment across all three epochs, particularly along the steep margins of the Fennoscandian shield and the Atlantic shelf break. Quantitative spatial analysis confirms this alignment, with mean nearest-neighbour offsets of 30.7 km at 8 ka, 62.9 km at 12 ka, and 89.3 km at 21 ka. The 95th-percentile Hausdorff distances are 433.0 km, 272.5 km, and 344.9 km, respectively. These mean offsets are on the order of the ∼50 km spatial resolution of the ICE-6G_C model used for the GIA deformation (Peltier et al., 2015), indicating robust paleo-reconstruction.

6.3. Benchmark comparison

We verified three well-documented paleogeographic events (Table 7):

7. Discussion and conclusions

7.1. Limitations

Several limitations should be considered when using PaleoEurope-DEM products:

1. **GIA model resolution.** The ICE-6G_C model is defined on a 10-arcminute grid (∼18 km). The GIA delta field (Eq. 10) is therefore spatially smooth, and fine-scale differential subsidence or uplift (e.g., due to local sediment loading or tectonics) is not captured. The effective vertical accuracy of the paleo-DEM is limited by the GIA model, not by the 30 m DEM resolution.
2. **Ice-sheet margins.** The ICE-7G_NA ice thickness is defined at 1° (∼111 km) resolution. Ice margins are therefore approximate, and the Envelope Method transition zone (Section 3.3) may not align precisely with geological evidence of moraine positions. Furthermore, when the coarse ICE-7G grid is resampled to the 30 m DEM resolution via bicubic interpolation, the ice thickness transitions linearly (or as a smooth ramp) between the model's grid nodes, rather than following the parabolic profile expected from physically based near-margin ice-flow models. We deliberately do not post-process the resampled ice field with an SIA profile correction, because doing so would introduce ice-thickness values not present in the source model, violating the data-provenance principle of the pipeline—which is designed to integrate, not synthesise, existing palaeoglacial reconstructions. Users interpreting fine-scale ice-surface topography in the marginal zone ($H_{\mathrm{ice}} < T_{\mathrm{tr}}$) should treat the linear ramp as an artefact of source-model resolution, not of the Envelope Method itself.
3. **GEBCO uncertainty on shelves.** Substantial portions of the North Sea and Baltic shelves in GEBCO are interpolated from sparse soundings (TID = 40), and the true seafloor elevation in these areas is uncertain. This affects the accuracy of paleotopographic features on exposed shelves.
4. **Coastal geomorphology distortion.** As noted in Section 3.1.4, the 300 m alpha-blending window used to fuse FABDEM and GEBCO locally distorts high-frequency coastal features (e.g., cliffs and barrier beaches). This trade-off ensures global surface continuity required for routing models but compromises local geomorphological precision at the land–sea interface.
5. **No explicit eustatic sea-level application.** Eustatic sea-level change is already embedded in the ICE-6G_C `Orog` field via the self-consistent GIA calculation. We do not apply a separate sea-level curve, which means the paleo-surfaces are internally consistent with the GIA model but may differ from independent sea-level reconstructions (Spratt and Lisiecki, 2016) by up to ∼10 m, depending on the epoch and region.
6. **Geoid correction sign.** The production pipeline supports an optional EGM2008-based undulation

offset applied to GEBCO ($Z_{\text{corr}} = Z_{\text{GEBCO}} - N$) when explicitly enabled. The sign convention must remain consistent between the manuscript and the implementation, but the appropriateness of applying any geoid offset depends on the datasets' effective vertical references and must be validated.

7.2. Comparison with existing approaches

Wickert (2016) produced flow-routing-capable paleo-DEMs for North America using ICE-5G. PaleoEurope-DEM v1.0 operates at 30 m, enabling identification of individual valleys, ridges, and channels on exposed shelves. However, Wickert (2016)'s approach includes dynamic ice-sheet routing, which is beyond the scope of the present work.

The total processing time for 3 150 tiles × 3 epochs was approximately 6.1 h on a two-node workstation cluster (1 h 07 min fusion + 5 h 04 min GIA application), demonstrating that continental-scale paleo-DEM generation is feasible without access to high-performance computing facilities. The total storage requirement was 744 GB (189 GB modern + 555 GB paleo epochs).

7.3. Potential applications

The generated paleo-DEMs can serve as input for: paleohydrological flow routing and drainage network extraction, archaeological site prediction on exposed continental shelves, paleoclimate model downscaling and boundary conditions, and coastal hazard assessment through comparison of paleo- and present-day coastlines.

7.4. Future work

In ongoing work, we extend the pipeline with a topological analysis stage using persistent homology to detect paleochannels in the deformed DEMs. Additional planned extensions include: support for higher-resolution GIA models as they become available, global domain extension, and coupling with surface process models.

7.5. Conclusions

We have presented PaleoEurope-DEM v1.0, an open-source distributed pipeline that produces 30 m-resolution paleo-DEMs for Europe at arbitrary epochs from 0 to 26 ka BP. The pipeline fuses FABDEM land topography with GEBCO bathymetry using alpha blending and evaluates an optional EGM2008-based geoid offset when validated, applies ICE-6G_C GIA deformation via a delta method that preserves fine-scale terrain detail, and models ice-sheet surfaces using a novel Envelope Method. The modular, containerized architecture enables reproducible execution on modest hardware. All code is publicly available under an MIT

license at https://github.com/archerby/paleoeurope, and the archived release is available on Zenodo (DOI: 10.5281/zenodo.18804506).

Acknowledgments

The author thanks the teams responsible for the open datasets used in this study: FABDEM (Hawker et al., University of Bristol), GEBCO (GEBCO Compilation Group), ICE-6G_C and ICE-7G_NA (W.R. Peltier and co-workers, University of Toronto), EGM2008 (National Geospatial-Intelligence Agency), Spratt & Lisiecki sea-level stack, and the PaleoMAP PaleoCoastlines dataset (Kocsis & Scotese). No external funding was received for this work.

Code availability

Name: PaleoEurope-DEM

Developer: Pavel Novikau

Contact: pavel@novikau.me

Hardware: x86-64 Linux workstation cluster (2 nodes, 20 cores total, 74 GB RAM)

Language: Python 3.11

Dependencies: GDAL 3.7+, Rasterio 1.3+, Celery 5.3+, SciPy 1.11+, NumPy, Redis 7.x

License: MIT

Repository: https://github.com/archerby/paleoeurope

API Documentation: https://archerby.github.io/paleoeurope-dem

Size: ∼3 GB (including pre-processed notebooks and figures)

Data availability

The input datasets used in this study are publicly available: FABDEM (Hawker et al., 2022), GEBCO 2024 (GEBCO Compilation Group, 2024), ICE-6G_C (VM5a) (Peltier et al., 2015), ICE-7G_NA (VM7) (Roy and Peltier, 2018), EGM2008 (Pavlis et al., 2012), and GSHHG (Wessel and Smith, 1996). Processed DEM products (derived rasters used for the figures and validation) have been archived on Zenodo (DOI: 10.5281/zenodo.18804506).

References

Björck, S., 1995. A review of the history of the Baltic Sea, 13.0–8.0 ka BP. Quaternary International 27, 19–40. doi:10.1016/1040-6182(94)00057-C.

Borgohain, A., Khajuria, V., Garg, V., Koti, S.R., Bhardwaj, A., 2023. Comparison of geomorphological parameters detected using merit and fabdem products. ECWS-7 2023 , 59doi:10.3390/ecws-7-14298.

Celery Project, 2024. Celery: Distributed task queue. https://docs.celeryq.dev/. Version 5.3+.

Dandabathula, G., Hari, R., Ghosh, K., Bera, A.K., Srivastav, S.K., 2022. Accuracy assessment of digital bare-earth model using icesat-2 photons: analysis of the fabdem. Modeling Earth Systems and Environment 9, 2677–2694. doi:10.1007/s40808-022-01648-4.

GEBCO Compilation Group, 2024. GEBCO_2024 Grid. https://www.gebco.net/data-products-gridded-bathymetry-data/gebco2024-grid. doi:10.5285/1c44ce99-0a0d-5f4f-e063-7086abc0ea0f.

Gupta, S., Collier, J.S., Garcia-Moreno, D., Oggioni, F., Trentesaux, A., Vanneste, K., De Batist, M., Camelbeeck, T., Potter, G., Van Vliet-Lanoë, B., Arthur, J.C.R., 2017. Two-stage opening of the Dover Strait and the origin of island Britain. Nature Communications 8, 15101. doi:10.1038/ncomms15101.

Guth, P.L., Geoffroy, T.M., 2021. Lidar point cloud and icesat-2 evaluation of 1 second global digital elevation models: Copernicus wins. Transactions in GIS 25, 2245–2261. doi:10.1111/tgis.12825.

Hawker, L., Uhe, P., Paulo, L., Sosa, J., Savage, J., Sampson, C., Neal, J., 2022. A 30 m global map of elevation with forests and buildings removed. Environmental Research Letters 17, 024016. doi:10.1088/1748-9326/ac4d4f.

Ho, Y.F., Grohmann, C.H., Lindsay, J., Reuter, H.I., Parente, L., Witjes, M., Hengl, T., 2025. Gedtm30: global ensemble digital terrain model at 30 m and derived multiscale terrain variables. PeerJ 13, e19673. doi:10.7717/peerj.19673.

Kageyama, M., Albani, S., Braconnot, P., Harrison, S.P., Hopcroft, P.O., Ivanovic, R.F., Lambert, F., Marti, O., Peltier, W.R., Peterschmitt, J.Y., Roche, D.M., Tarasov, L., Zhang, X., Brady, E.C., Haywood, A.M., LeGrande, A.N., Lunt, D.J., Mahowald, N.M., Mikolajewicz, U., Nisancioglu, K.H., Otto-Bliesner, B.L., Renssen, H., Tomas, R.A., Zhang, Q., Abe-Ouchi, A., Bartlein, P.J., Cao, J., Li, Q., Lohmann, G., Ohgaito, R., Shi, X., Volodin, E., Yoshida, K., Zhang, X., Zheng, W., 2017. The PMIP4 contribution to CMIP6 – Part 4: Scientific objectives and experimental design of the PMIP4-CMIP6 Last Glacial Maximum experiments and PMIP4 sensitivity experiments. Geoscientific Model Development 10, 4035–4055. doi:10.5194/gmd-10-4035-2017.

Kocsis, Á.T., Scotese, C.R., 2021. Mapping paleocoastlines and continental flooding during the phanerozoic. Earth-Science Reviews 213, 103463. doi:10.1016/j.earscirev.2020.103463.

Kocsis, Á.T., Scotese, C.R., 2023. PaleoMAP PaleoCoastlines data (7.2). https://zenodo.org/records/7828387. doi:10.5281/zenodo.7828387. data set, CC-BY-4.0.

Marsh, C.B., Harder, P., Pomeroy, J.W., 2023. Validation of FABDEM, a global bare-earth elevation model, against UAV-lidar derived elevation in a complex forested mountain catchment. Environmental Research Communications 5, 031009. doi:10.1088/2515-7620/acc56d.

Meadows, M., Jones, S., Reinke, K., 2024. Vertical accuracy assessment of freely available global dems (fabdem, copernicus dem, nasadem, aw3d30 and srtm) in flood-prone environments. International Journal of Digital Earth 17. doi:10.1080/17538947.2024.2308734.

Müller, R.D., Cannon, J., Qin, X., Watson, R.J., Gurnis, M., Williams, S., Pfaffelmoser, T., Seton, M., Russell, S.H.J., Zahirovic, S., 2018. GPlates: Building a virtual Earth through deep time. Geochemistry, Geophysics, Geosystems 19, 2243–2261. doi:10.1029/2018GC007584.

Pavlis, N.K., Holmes, S.A., Kenyon, S.C., Factor, J.K., 2012. The development and evaluation of the Earth Gravitational

Model 2008 (EGM2008). Journal of Geophysical Research: Solid Earth 117, B04406. doi:10.1029/2011JB008916.

Peltier, W.R., Argus, D.F., Drummond, R., 2015. Space geodesy constrains ice age terminal deglaciation: The global ICE-6G_C (VM5a) model. Journal of Geophysical Research: Solid Earth 120, 450–487. doi:10.1002/2014JB011176.

Roy, K., Peltier, W.R., 2018. Relative sea level in the Western Mediterranean basin: A regional test of the ICE-7G_NA (VM7) model and a constraint on late Holocene Antarctic deglaciation. Quaternary Science Reviews 183, 76–87. doi:10.1016/j.quascirev.2017.12.021.

Spratt, R.M., Lisiecki, L.E., 2016. A Late Pleistocene sea level stack. Climate of the Past 12, 1079–1092. doi:10.5194/cp-12-1079-2016.

Wessel, P., Smith, W.H.F., 1996. A global, self-consistent, hierarchical, high-resolution shoreline database. Journal of Geophysical Research: Solid Earth 101, 8741–8743. doi:10.1029/96JB00104.

Wickert, A.D., 2016. Reconstruction of North American drainage basins and river discharge since the Last Glacial Maximum. Earth Surface Dynamics 4, 831–869. doi:10.5194/esurf-4-831-2016.